Eur. Phys. J. B (2015) 88: 192
DOI: 10.1140/epjb/e2015-60053-2

THE EUROPEAN PHYSICAL JOURNAL B

Regular Article

Jamming mechanism on the scale-free network with heterogeneous node capacity

Yup Kim[a], Hyunjun Park, Woosik Choi, and Soon-Hyung Yook[b]

Department of Physics and Research Institute for Basic Sciences, Kyung Hee University, Seoul 130-701, Korea

Received 16 January 2015 / Received in final form 15 June 2015
Published online 3 August 2015 –

Abstract. To understand how the jamming on real communication networks depends on node capacity, we study the traffic model with heterogeneous node capacity. In this model, each movable packet takes a biased random walk and the capacity of a node with degree k is given as $C(k) \sim k^x$ with a tunable parameter x. Each packet disappears when it arrives at the preassigned target node. We analytically and numerically show that the transition from the free-flow phase to the jammed phase occurs when the balance between the packet generations and removals is broken. The balance breaking condition for the jamming is analytically determined by the competition between $C(k)$ and the average number of packets on a node of degree k, $m_f(k)$, in the free-flow phase. Based on the analytic arguments, we find that there exist three different jamming patterns depending on $C(k)$. The analytic conjectures for jamming patterns are verified by numerical simulations.

1 Introduction

Due to the explosive growth of the global communication networks for last two decades, such as the Internet [1] and world-wide-web [2], understanding the dynamical processes for the information flow over the networks becomes more important than before. Such dynamical processes are closely related to the navigability [3], the efficient information searching algorithms [4–7], and the optimal routing strategy [8–15]. The navigability of network means the ability to reach any given node starting from any other node. To determine the navigability, a message (or a packet) is produced at a randomly chosen node and forwarded to an arbitrarily selected node with greedy algorithm in general. In the information search, query packets generated at any node explore the network until they find the requested information according to a given packet forwarding rule. In these studies, there is an important common dynamical process shared by the suggested models, i.e., a packet generated on a node is forwarded to one of its linked neighbors under a given dynamic rule, which is generally referred as a routing rule. Therefore, understanding the packet forwarding rules is essential to study the dynamical properties of information flow in real networks.

The packet forwarding rules can be classified into two different types depending on the used information to move a packet to a neighboring node. The first type of the packet forwarding rule uses the global information, such as the shortest path between the nodes [3,9], betweenness centrality [10], and optimal packet flow pattern [11]. Even though this type of packet forwarding rule is the best one among others, it may be practical for only small size of networks because of the increasing computational complexity and resources. Additionally, in many real networks, acquiring the global information of the underlying network is limited because of, for example, incomplete sampling [16]. In order to avoid such difficulties the models based on the local information are suggested as the other type of packet forwarding rule. One of the most popular models for this type of packet forwarding rule is the random walk. Due to its theoretical importance and wide range of application, various dynamical properties of random walks on complex networks are well studied [17–19].

In real communication networks, there normally exist huge number of packets on the network. At each time, new packets are generated, then move toward the target nodes. When the packet arrives at the target node, the packet is removed. If the number of new generated packets does not balance with that of removed packets, then the traffic congestion occurs and sometimes the network loses its function. Therefore, the traffic is a very important factor to be considered to design and control the information flow over the network. The traffic on the network is also closely related to well-known physics problems. For example, we have shown that the efficiency of the peer-to-peer network protocol can be drastically improved by exploiting the diffusive capture process for information search [6,7].

Recently, Wang et al. suggested a biased random walk (BRW) routing model to find an optimal condition for the local information based packet forwarding strategy [12,13]. In this model, each node has the same fixed capacity, C,

[a] e-mail: ykim@khu.ac.kr
[b] e-mail: syook@khu.ac.kr

which is the maximum number of simultaneously movable packets on a node. At each time R packets are generated at the randomly selected nodes. Each movable packet takes BRW to one of the connected nodes of degree k with the hopping probability proportional to k^α. In addition they applied the path iteration avoidance (PIA) rule to increase the efficiency. Under the PIA rule a packet cannot visit each link more than twice. From the numerical simulations, they showed that the model undergoes a transition from the free-flow phase to the jammed phase as R increases. In addition, they also found that the transition threshold, R_c, depends on α and becomes the maximum when $\alpha = -1$. Based on the analysis of the behavior of $R_c(\alpha)$, they suggested that $\alpha = -1$ is the optimal parameter for BRW routing model with PIA. Even though the imposed PIA rule has practical implication by increasing R_c, we find that it is not a relevant factor to determine the transition pattern. BRW is also used to find the optimal diffusion process on a network which maximizes the entropy rate of the Markov chain [20–22]. The maximal-entropy walk includes the limiting case of BRW routing model with infinite capacity ($C = \infty$). In the maximal-entropy walk, the optimal diffusion process is obtained when $\alpha = 1$ for uncorrelated networks, at which the walkers are maximally dispersed on all possible paths.

However, in real networks, each node has different packet forwarding capacity. Thus, it is very important to understand how the heterogeneity in C affects on the physical origin of jamming and how the jammed phase occurs in the system as R increases. Therefore, in this paper, we introduce the BRW routing model with topology-dependent node capacity to study the effect of the heterogeneous capacity on the patterns of jamming. For this purpose, we consider the degree-dependent node capacity,

$$C = C(k) = ck^x. \tag{1}$$

Here x is a tunable parameter and c is a constant. It is very natural assumption because in many communication networks the nodes of the large degree belong to the (commercial) service providers. In general such service providers should have equipment of large capacity for reliable service. From analytic arguments, we show that there are three different jamming patterns depending on x and α. When $\alpha + 1 > x$ we find that the jamming mechanism is exactly the same as the condensation mechanism in the zero range process on complex networks [23]. In contrast, jamming patterns for $\alpha + 1 \leq x$ show peculiar behaviors, which have never been studied in any other traffic models. When $\alpha + 1 < x$, we find that the congestion occurs from the nodes with smallest degree as R increases. When $\alpha + 1 = x$, the stacking of the packets occurs over all the nodes in the network for $R > R_c$. We verify all the analytic results through the numerical simulations. The results do not depend on the sign of x, i.e., x can be positive or negative. However, in the following simulations we show the numerical results for $x > 0$ to explain the jamming patterns on real networks as addressed above. In addition, BRW routing model in references [12,13] corresponds to the case of $x = 0$, thus the jamming pattern of BRW routing model with $\alpha = -1$ is exactly the same with the case of $x = \alpha + 1$.

2 Traffic model

As explained in introduction, the traffic model considered in this paper is nearly the same as that treated in references [12,13]. Therefore, we briefly explain the traffic model on networks for the clearness sake. In the model, at each time step, we perform the three following processes. (I) Generation process: R packets are generated from randomly chosen nodes on the network and we assign the destination node of each packet at random. (II) Hopping process: let N_i be the number of packets on node i with degree k_i, and let $C_i = \lfloor C(k_i) \rfloor$ where $\lfloor C(k_i) \rfloor$ is the largest integer which is less than or equals to $C(k_i) = ck_i^x$. If $N_i \leq C_i$ at a given time t, then all packets on i are movable. When $N_i > C_i$, C_i packets move and $(N_i - C_i)$ packets are stacked. To the selection of packets to move, we apply the FIFO (first in first out) discipline [14,15]. Selected packets simultaneously move at t. Each movable packet on a node i takes BRW with the hopping probability T_{ij} from i to one of the linked neighbors j [24–26] as:

$$T_{ij} = \frac{k_j^\alpha}{\sum_{\ell=1}^{k_i} k_\ell^\alpha}. \tag{2}$$

Here k_i is the degree of node i and $\sum_{\ell=1}^{k_i}$ denotes the sum over the linked neighbors of the node i. Since each node can identify all of its neighbors, it can pass the packet directly to the target if one of the linked neighbors is the preassigned target node. (III) removal process: once a packet arrives at its destination, it disappears from the network.

BRWs depend on the parameter α. $\alpha = 0$ means that the walk reduces to normal random walks. $\alpha > 0$ (<0) means the walk prefers the node with higher degree (lower degree). To analyze the dependence of physical origin of the jamming patterns on C_i as emphasized in Introduction, we assume that C_i in our model depends on the network topology, i.e., the degree k_i of the node i, in a variety of ways.

3 Node capacity and Jamming patterns

We now want to explain the dependence of jamming mechanisms on the node capacity C_i in the traffic model. To reflect the traffic properties in the real system, we consider the scale-free network (SFN) with the degree distribution $P_d(k) \sim k^{-\gamma}$ and the size N. We assign the capacity of node i as $C_i = C(k_i) = ck_i^x$.

In order to analyze the traffic model on the base network, the order parameter [27,28],

$$\eta(R) = \lim_{t\to\infty} \frac{1}{R} \frac{\langle \Delta N_p \rangle}{\Delta t}, \tag{3}$$

is used. Here, $\Delta N_p = N_p(t + \Delta t) - N_p(t)$ and $N_p(t)$ represents the number of packets on the network at time t.

$\langle \ldots \rangle$ indicates average over time windows of width Δt. In the free-flow phase in which $\eta(R) = 0$, $\langle \Delta N_p \rangle = 0$, i.e., $N_p(t)$ does not vary. Thus, the free-flow phase means a sort of stationary state with the balance between generated packets and removed packets [12]. In the free-flow phase, the probability $P_b(k)$ that a randomly chosen packet which does BRW with equation (2) is found at a node with degree k is [20,25]

$$P_b(k) = \frac{k^{\alpha+1}}{N \langle k^{\alpha+1} \rangle}. \quad (4)$$

$P_b(k)$ is the biased-random-walk centrality. Thus, the average number, $m_f(k)$, of packets on the nodes with degree k in the free-flow phase becomes $m_f(k) = \frac{N_p k^{\alpha+1}}{N \langle k^{\alpha+1} \rangle}$. Since N_p should be proportional to R (or $N_p = ANR$) in the free-flow phase, $m_f(k)$ can be written as

$$m_f(k) = \frac{N_p k^{\alpha+1}}{N \langle k^{\alpha+1} \rangle} = aRk^{\alpha+1}, \quad (5)$$

where A is a proportional constant and $a = A / \langle k^{\alpha+1} \rangle$.

However, as packets entering in the system increase or R increases, the jammed phase, $\eta(R) > 0$, occurs for $R > R_c$ [12,13]. In the jammed phase the number of generated packets becomes unbalanced with that of removed packets. The balance is determined by the node capacity $C(k)$. Thus, patterns of mechanisms for the jammed phase should be analyzed by the competition between $C(k)$ and $m_f(k)$ as shown in Figure 1.

When $C(k) > m_f(k)$ on all nodes, any packet on any node freely moves to its neighboring nodes, and sooner or later it arrives at its destination node without jamming. So, the number of generated packets balances with that of removed packets in the steady state. Therefore, when $C(k) > m_f(k)$ for any k, the state is in the free-flow phase. In contrast, when $C(k) < m_f(k)$ for a certain k, some packets on the node with degree k cannot move and such immovable packets should be stacked on the node. These stacks make $\langle \Delta N_p \rangle > 0$, i.e., the jammed phase ($\eta(R) > 0$). Therefore, one can classify jamming patterns by the comparison between $C(k)$ and $m_f(k)$ as shown in Figure 1.

We first consider the case of $\alpha + 1 > x$ as shown in Figure 1a. The degree k of the SFN with the size N is in the interval $[k_{\min}, k_{\max}]$. Here $k_{\min}$ is the minimum degree which does not depend on N. $k_{\max}$ is the maximum degree in the network which scales as $k_{\max} \sim N^{1/(\gamma-1)}$ if we do not impose any artificial cutoff [29]. As R increases in the free-flow phase, the average packet number $m_f(k)(=aRk^{\alpha+1})$ on the nodes with degree k increases. When R reaches to the threshold, R_c, $m_f(k)$ first meets $C(k)$ at $k_{\max}$ as shown in Figure 1a. Thus, the jammed phase begins to occur when R satisfies the relation $m_f(k_{\max}) = aRk_{\max}^{\alpha+1} = C(k_{\max}) = ck_{\max}^{x}$ or $R = R_c = ca^{-1}k_{\max}^{x-\alpha-1}$. When $R = R_c^+$ (or $R \to R_c$ from above), the jamming occurs only on the node with degree $k_{\max}$ (hub node), because the condition $C(k) > m_f(k)$ that any packet on the node freely moves first breaks on the hub node. Since $k_{\max} \sim N^{1/(\gamma-1)}$, the critical value of

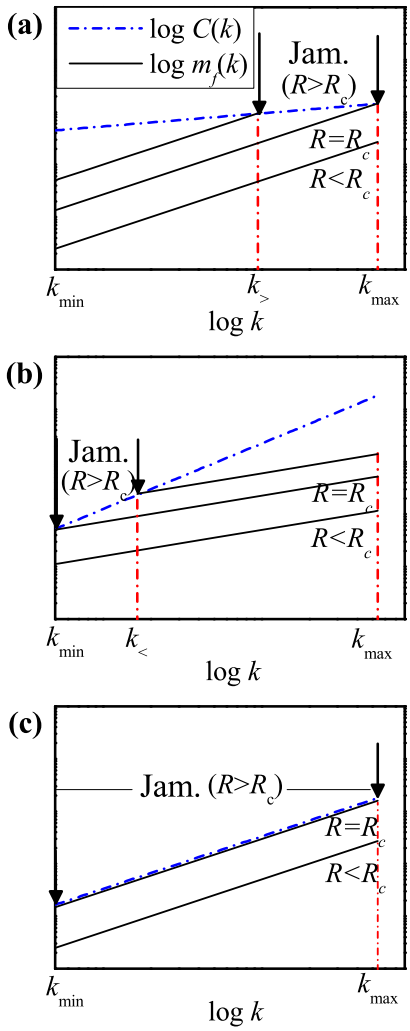

Fig. 1. The schematic illustrations for jamming patterns (a) when $\alpha + 1 > x$, (b) when $\alpha + 1 < x$, and (c) when $\alpha + 1 = x$. Solid line denotes the $m_f(k)$ for a given R and dash-dotted (blue) line denotes the node capacity, $C(k)$. "Jam." means the range of k in which jamming occurs for a given $R(> R_c)$.

R, R_c, depends on N as

$$R_c(N) \propto N^{\beta} \left(\beta = \frac{x - \alpha - 1}{\gamma - 1} \right). \quad (6)$$

The jammed phase in which η has non-zero value occurs for $R > R_c$. When $R > R_c$, jamming occurs on the nodes with degree $k \geq k_>$ as shown in Figure 1a. Here $k_>$ is the smallest value of k at which jamming occurs. On the nodes with degree $k \geq k_>$, the free BRW condition $C(k) > m_f(k)$ breaks. $k_>$ depends on N and R in the complex way, because the number of jammed packets on the nodes with $k \geq k_>$, $\sum_{k_>}^{k_{\max}} m(k)$, is not known. Here, $m(k)$ is the average number of packets on the nodes with k. In contrast, the jamming does not occur on the nodes with $k < k_>$. Therefore, in the case of $\alpha + 1 > x$, the jamming pattern is that the jamming for a given $R(>R_c)$ occurs on the nodes with $k \geq k_>(R)$ or with the higher degree.

In the case of $\alpha+1<x$ shown in Figure 1b, the jamming pattern is changed. In this case, when R reaches R_c from the free-flow phase, $m_f(k)$ first meets $C(k)$ at $k_{\min}$ as illustrated in Figure 1b. Thus, the jammed phase begins to occur when R satisfies the relation $m_f(k_{\min})=aRk_{\min}^{\alpha+1}=C(k_{\min})=ck_{\min}^{x}$ or $R=R_c=ca^{-1}k_{\min}^{x-\alpha-1}$. Since $k_{\min}$ does not depend on the size N, R_c does not depend on N. When $R=R_c^+$, the jamming occurs on the nodes with degree $k_{\min}$, because the condition $C(k)>m_f(k)$ breaks on the nodes with degree $k_{\min}$. The jammed phase in which η has non-zero value occurs for $R>R_c$ as in the case of $\alpha+1>x$. When $R>R_c$, jamming occurs on the nodes with degree $k\le k_<$ as shown in Figure 1b. Here $k_<$ is the largest degree at which jamming occurs. On the nodes with degree $k\le k_<$, the free BRW condition $C(k)>m_f(k)$ breaks. In contrast, the jamming does not occur on the nodes with $k>k_<$. $k_<$ also depends on N and R in the complex way because the number of jammed packets on the nodes with $k\le k_<$, $\sum_{k_{\min}}^{k_<}m(k)$, is also not analytically tractable as in the case of $\alpha+1>x$. Therefore, in the case of $\alpha+1<x$, the jamming pattern is that the jamming for a given $R(>R_c)$ occurs on the nodes with $k\le k_<(R)$ or with the lower degree.

Finally, we illustrate the jamming pattern for the case of $\alpha+1=x$ in Figure 1c. The jammed phase begins to occur when R satisfies the relation $m_f(k)=aRk^{\alpha+1}=C(k)=ck^x$ or $R=R_c=ca^{-1}$. Therefore, R_c does not depend on $k_{\min}$, $k_{\max}$, and N. Unlike the cases of $x>\alpha+1$ and $x<\alpha+1$, the condition $C(k)>m_f(k)$ simultaneously breaks on all nodes (or for all k) and the jamming also begins to occur on all nodes when $R=R_c^+$. For $R>R_c$, packets are also stacked on any node. Therefore, in the case of $\alpha+1=x$, the jamming pattern is that the jamming for a given $R(>R_c)$ simultaneously occurs on all nodes.

4 Confirming simulations

To confirm the jamming patterns suggested in the previous section, we perform the simulation for the traffic model on the SFN. In the following simulations we use Barabási and Albert (BA) network with the average degree $\langle k\rangle=10$ and $k_{\min}=5$ as a underlying topology [30]. BA network has the degree distribution $P_d(k)\sim k^{-\gamma}$ with $\gamma=3$. We also check our results using SFNs with other γ's and find nearly the same results as those on BA network. Used network sizes are $N=10^4$, 2×10^4, 4×10^4 and 8×10^4. We average the simulation data over 3000 realizations of SFNs with a given N.

4.1 Jamming in the case of $\alpha+1>x$

In Figure 2, we show the simulation results for the traffic model with $(c=20,x=0,\alpha=0)$ and $(c=20,x=1/4,\alpha=1/2)$, respectively, to justify the conjectured jamming pattern for $\alpha+1>x$. The obtained $\eta(R)$'s are displayed in the insets of Figures 2a and 2b, which are nearly identical to that in references [12,13]. $\eta(R)$ from the simulation confirms well the transition from the free-flow phase $(\eta(R)=0)$ for $R<R_c$ to the jammed phase $(\eta(R)>0)$ for $R>R_c$. Since $R_c(N)\simeq N^{\beta}$ $(\beta=(x-\alpha-1)/(\gamma-1))$ from equation (6), $\eta(R)$ should scale with N as $\eta(R)=f(R/N^{\beta})$. For the network with $\gamma=3$, we obtain $\beta=-1/2$ if $(x=0,\alpha=0)$, and $\beta=-5/8$ if $(x=1/2,\alpha=1/4)$. As shown in Figures 2a and 2b, the simulation results confirm the scaling of $\eta(R)$ very well and the conjectured jamming pattern in Section 3.

We also measure the average number $m(k)$ of packets for $R\simeq R_c(N)$ at $t=10N$ as the insets of Figures 2c and 2d. Except for $k=k_{\max}$, measured $m(k)$'s satisfy $m(k)=m_f(k)\propto k^{\alpha+1}=k^1$ when $\alpha=0$, and $m(k)=m_f(k)\propto k^{3/2}$ when $\alpha=1/2$. The results show a good agreement with equation (5). If the conjectured jamming pattern in the case of $\alpha+1>x$ is right, jamming appears at $k=k_{\max}$ for $R\simeq R_c$. The insets of Figures 2c and 2d also clearly show that the jamming occurs on the node with $k=k_{\max}$ when $R\simeq R_c$. Since the jamming occurs on the node with $k=k_{\max}$ at $R\simeq R_c(N)$, $m(k)$ scales as $m(k_{\max})=m_f(k_{\max})=aR_c(N)k_{\max}^{\alpha+1}\sim cN^{x/(\gamma-1)}$ for $k=k_{\max}$, and $m(k)=m_f(k)=aR_c(N)k^{\alpha+1}\sim cN^{\beta}k^{\alpha+1}$ for $k<k_{\max}$. From these relations, we expect that $m(k)$ would scale with N as:

$$m(k)=N^{x/(\gamma-1)}g\left(k/N^{1/(\gamma-1)}\right), \tag{7}$$

at $R\simeq R_c$. Here the function g satisfies

$$g\left(k/N^{1/(\gamma-1)}\right)=\text{const.} \qquad \text{for } k=k_{\max}$$

and

$$g\left(k/N^{1/(\gamma-1)}\right)\sim\left[k/N^{1/(\gamma-1)}\right]^{\alpha+1} \qquad \text{for } k<k_{\max}.$$

Thus, for $(x=0,\ \alpha=0)$ $m(k)$ scales as $m(k)/N^0\sim cN^{-1/2}k^1$ when $k<k_{\max}$, and $m(k_{\max})/N^0=$ const. when $k=k_{\max}$ as shown in Figure 2c. Similarly, for $(x=1/4,\ \alpha=1/2)$ $m(k)$ satisfies $m(k)/N^{1/8}\sim c(N^{-1/2}k)^{3/2}$ when $k<k_{\max}$, and $m(k_{\max})/N^{1/8}=$ const. when $k=k_{\max}$ as in Figure 2d.

This jamming pattern at $R=R_c^+$ is exactly the same as the condensation on the hub node in the zero range process (ZRP) on SFN [23], because $m(k)$ in ZRP is the same as that in the insets of Figures 2c and 2d. In ZRP, if the given number N_p of particles is larger than $\sum_{k=k_{\min}}^{k_{\max}}m_f(k)$, then the excess number of particle, $N_p-\sum_{k=k_{\min}}^{k_{\max}}m_f(k)$, condenses on the hub node. This mechanism of condensation in ZRP is exactly the same jamming mechanism of the traffic model on SFNs.

In Figures 2e and 2f, we show the time dependence of measured $m(k)$ at $R\simeq R_c$ (or $R=R_c^+$) on the SFN with $N=10^4$. Except $m(k_{\max})$, $m(k)$ does not vary with the time t and $m(k)=m_f(k)$. In contrast, $m(k_{\max})$ increases with t, because jamming occurs only on the hub node and the jammed packets increases with t. To confirm the jamming pattern for $R>R_c$, we measure $m(k)$ for $R>R_c$ (see Figs. 2g and 2h). As expected the jamming occurs on the nodes with degree $k\ge k_>$. In contrast, the jamming does not occur and $m(k)$ scales as $k^{\alpha+1}$ on the nodes with

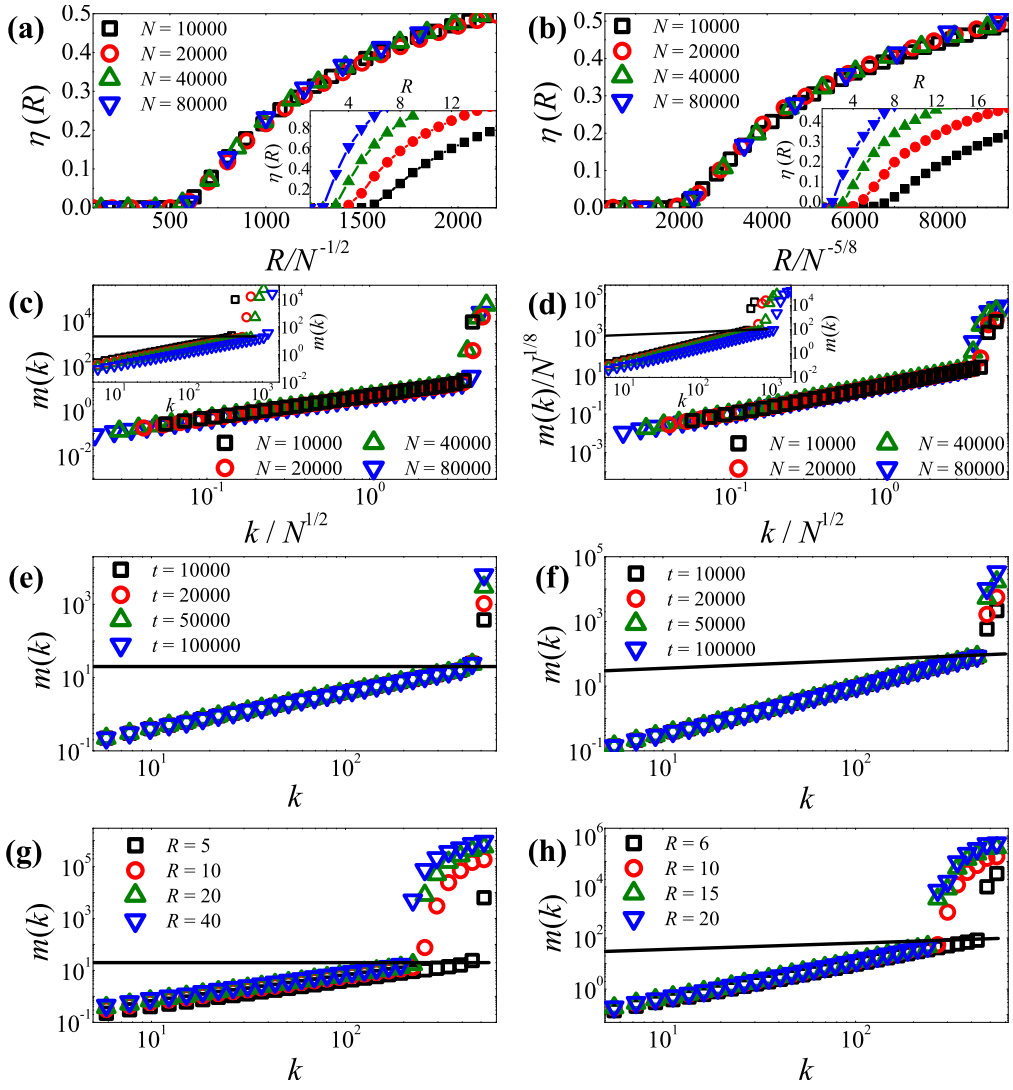

Fig. 2. Simulation results for $\alpha + 1 > x$. (a), (c), (e), and (g) are the case of ($\alpha = 0$, $x = 0$, $c = 20$). (b), (d), (f), and (h) correspond to the case of ($\alpha = 1/2$, $x = 1/4$, $c = 20$). (a), (b) The scaling plots of η against R/N^{β} with (a) $\beta = -1/2$ and with (b) $\beta = -5/8$. Insets: measured order parameter η against R. Obtained R_c's are (a) $R_c = 5, 4, 3, 2$ and (b) $R_c = 6, 4, 3, 2$ for $N = 10^4, 2 \times 10^4, 4 \times 10^4, 8 \times 10^4$. (c), (d) The scaling plots of $m(k)$. Insets: Measured $m(k)$ for $R \simeq R_c$ at $t = 10N$. Solid lines represent the relation, $C(k) = 20k^x$. (e), (f) The plots of $m(k)$ against k for $N = 10^4$ with (e) $R = 5$ and (f) $R = 6$ at $t = 10^4, 2 \times 10^4, 5 \times 10^4$, and 10^5. (g), (h) Plots of $m(k)$ against k for $N = 10^4$ with (g) $R = 5, 10, 20, 40$ and (h) $R = 6, 10, 15, 20$. On the nodes with the degree $k < k_>$, $m(k)$ shows the behavior with $m(k) \simeq m_f(k) \sim k^{\alpha+1}$. In contrast, jamming occurs on the nodes with $k \geq k_>$. $k_>$ decreases with $R(> R_c)$.

$k < k_>$. Thus, the conjectured jamming pattern for the case of $\alpha + 1 > x$ in the previous section is confirmed by the simulations of the traffic model with $(\alpha = 0, x = 0)$ and $(\alpha = 1/2, x = 1/4)$. We also verify the conjectured pattern for $\alpha + 1 > x$ by the simulations of the models with $(\alpha = 0, x = 0.5)$ and $(\alpha = 1, x = 0.5)$. If this type of jamming pattern arises in the real network traffics, we should enhance the capacity $C(k)$ of the nodes with higher degree or $k \geq k_>$ to avoid the jamming.

4.2 Jamming in the case of $\alpha + 1 < x$

In Figure 3 we show the simulation results for the traffic model with ($\alpha = 0$, $x = 3/2$, $c = 0.1$) and ($\alpha = -1/2$, $x = 1$, $c = 0.2$). The results show a good agreement with the conjectured jamming patterns in the case of $\alpha + 1 < x$. As in the case of $\alpha + 1 > x$, $\eta(R)$'s in Figures 3a and 3b show the transition from the free-flow phase to the jammed phase. R_c obtained from the simulation does not depend on N. This result supports the conjecture $R_c = ca^{-1}k_{\min}^{x-\alpha-1}$ in Section 3, because $k_{\min}$ does not depend on N. From the best fit of the relation $m_f(k) = aRk^{\alpha+1}$ to the data in the insets of Figures 3c and 3d, we obtain $a = 0.008(1)$ for $(\alpha = 0, x = 3/2)$ and $a = 0.04(1)$ for $(\alpha = -1/2, x = 1)$, respectively. When the value of R is fixed, large value of a means that N_p becomes large by the definition of a. Therefore, larger value of a provides smaller value of R_c. This can be verified by the

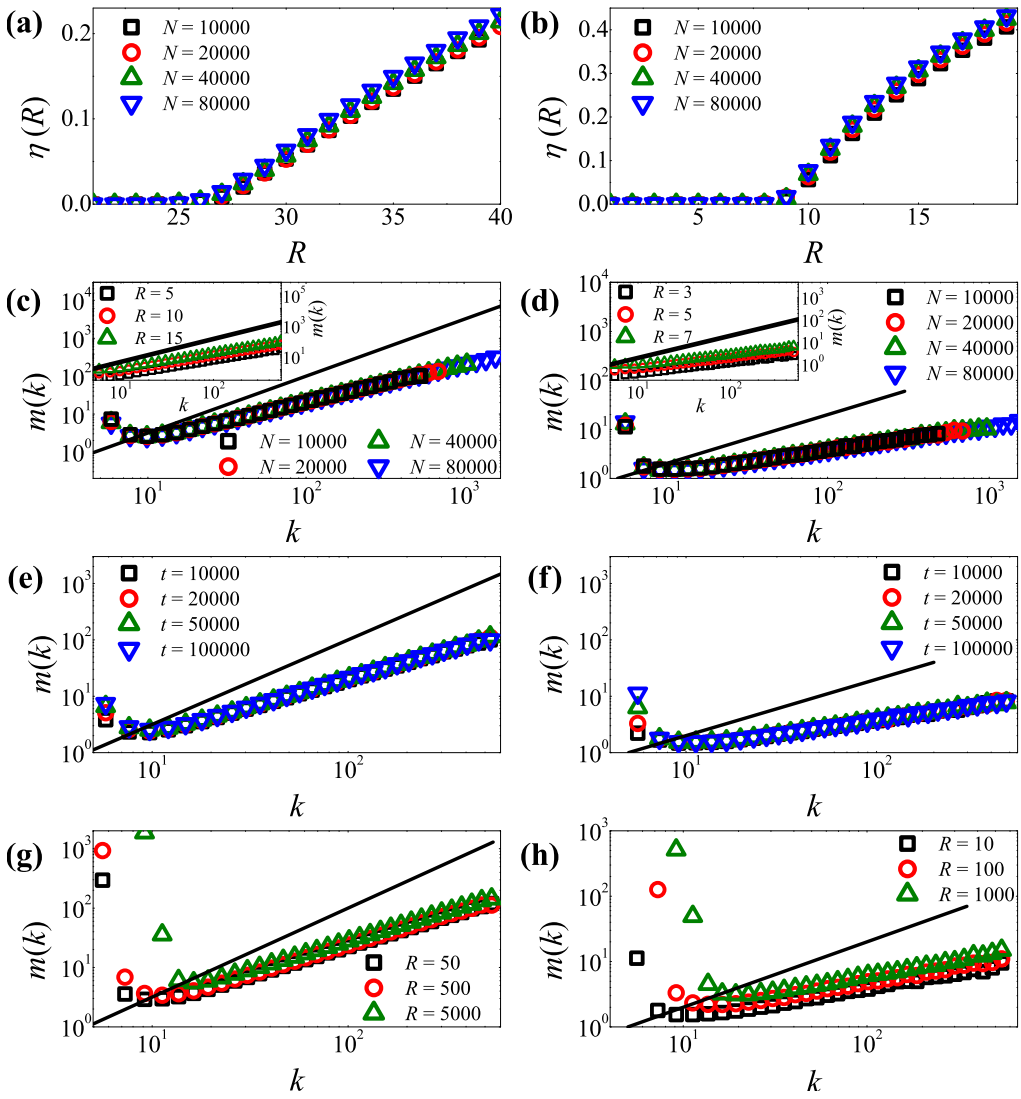

Fig. 3. Simulation results for $\alpha + 1 < x$. (a),(c),(e), and (g) are the case of $(\alpha = 0, x = 3/2, c = 0.1)$. (b),(d),(f), and (h) correspond to the case of $(\alpha = -1/2, x = 1, c = 0.2)$. (a), (b) The plots of order parameter η against R. Measured R_c's are (a) $R_c = 26(1)$ and (b) $R_c = 10(1)$, regardless of N. The plots of $m(k)$ for (c) $R = 26$ and (d) $R = 10$ at $t = 10N$. Solid lines denote (c) $C(k) = 0.1 \times k^{1.5}$ and (d) $C(k) = 0.2 \times k$. Insets: obtained $m(k)$ for $N = 10^4$ with (c) $R = 5, 10, 15$ $(< R_c)$, and (d) $R = 3, 5, 7$ $(< R_c)$. (e),(f) The plots of $m(k)$ against k for $N = 10^4$ at $t = 10^4, 2 \times 10^4, 5 \times 10^4$, and 10^5 with (e) $R = 26$ and (f) $R = 10$. (g),(h) The plots of $m(k)$ against k at $t = 10^5$ for $N = 10^4$ with (g) $R = 50, 500, 5000$ and (h) $R = 10, 100, 1000$. On the nodes with the degree $k > k_<$, $m(k)$ shows the behavior with $m(k) \simeq m_f(k) \sim k^{\alpha+1}$. In contrast, jamming occurs on the nodes with $k \leq k_<$. $k_<$ increases with $R(> R_c)$.

estimation of R_c through the analytic expression of R_c and numerical simulations. Using $a = 0.008(1)$ and $k_{\min} = 5$ for $(\alpha = 0, x = 3/2, c = 0.1)$, the theoretical value of R_c from $R_c = ca^{-1}k_{\min}^{1/2}$ is obtained as $R_c = 28(2)$, which is identical to the measured $R_c \simeq 26(1)$ from $\eta(R)$ within the estimated errors. Similarly, for $(\alpha = -1/2, x = 1, c = 0.2)$ we estimate $R_c = 11(2)$ from the analytic conjecture, which also coincides with the numerically obtained value $R_c \simeq 10(1)$ within the estimated errors. Furthermore, $\eta(R)$ for any R is the same regardless of N.

Figures 3c and 3d show the measured $m(k)$ at $R \simeq R_c$. If the conjectured jamming pattern in the case of $\alpha + 1 < x$ is right, jamming for $R \simeq R_c$ appears around $k = k_{\min} = 5$. In Figures 3c and 3d jamming occurs for $k \simeq 5$, which agrees with the theoretical expectation for $R \simeq R_c$. Except for $k \simeq 5$, measured $m(k)$'s satisfy the theoretical conjecture, $m(k) = m_f(k) \propto k^{\alpha+1}$ (see Eq. (5)). Figures 3e and 3f show the time dependence of measured $m(k)$'s at $R \simeq R_c$ on the SFN with $N = 10^4$. Except $m(k)$ for $k \simeq 5$, $m(k)$ does not vary with time t and $m(k) = m_f(k)$. In contrast, $m(k)$ for $k \simeq 5$ increases with t, because jamming occurs on the nodes with degree $k = 5$ and the jammed packets increase with t.

In Figures 3g and 3h we show the measured $m(k)$'s for $R > R_c$. As expected the jamming occurs only on the nodes with degree $k \leq k_<$. In contrast, the jamming

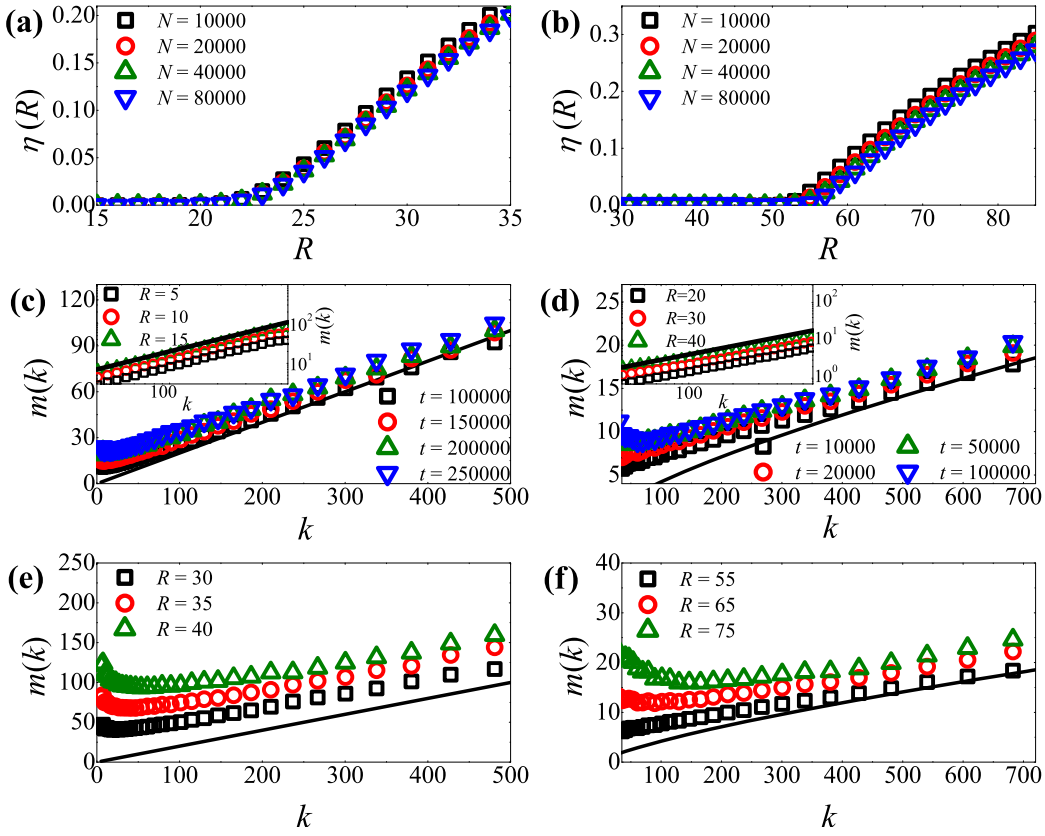

Fig. 4. Simulation results for the case of $\alpha+1=x$. (a), (c) and (e) show the results for $(\alpha=0, x=1, c=0.2)$. (b), (d) and (f) correspond to the case of $(\alpha=-1/4, x=3/4, c=0.133)$. (a),(b) The plots of order parameter η against R. Obtained R_c from $\eta(R)$ is (a) $R_c=24(1)$ and (b) $R_c=54(2)$, regardless of N. (c),(d) The plots of $m(k)$ against k with $N=10^4$ for (c) $R=24$ at $t=10^5, 1.5\times10^5, 2\times10^5$, 2.5×10^5, and (d) $R=54$ at $t=10^4, 2\times10^4, 5\times10^4, 10^6$. Solid lines denote (c) $C(k)=0.2\times k$ and (d) $C(k)=0.133\times k^{3/4}$. Insets: Measured $m(k)$ for (c) $R=5, 10, 15(<R_c)$ and (d) $R=20, 30, 40(<R_c)$ with $N=10^4$ at $t=10^5$. $m(k)$ for $R<R_c$ satisfies the relation (c) $m(k)=m_f(k)=aRk$ and (d) $m(k)=m_f(k)=aRk^{3/4}$. (e),(f) The plots of $m(k)$ against k for $N=10^4$ with (e) $R=30, 35, 40(>R_c)$ and (d) $R=55, 65, 75(>R_c)$ at $t=10^5$.

does not occur and $m(k)$ scales as $k^{\alpha+1}$ on the nodes with $k>k_<$. Thus, we verify the conjectured jamming pattern for the case of $\alpha+1<x$ in Section 3 through the numerical simulations with $(\alpha=0, x=3/2)$ and $(\alpha=-1/2, x=1)$. If this type of jamming pattern arises in the real network traffic, the capacity $C(k)$ of the nodes with lower degree or $k\le k_<$ should be enhanced more to avoid the jamming.

4.3 Jamming in the case of $\alpha+1=x$

Finally, to confirm the conjectured jamming pattern for $\alpha+1=x$, we also perform the simulations with $(\alpha=0, x=1, c=0.2)$ and $(\alpha=-1/4, x=3/4, c=0.133)$. $\eta(R)$'s in Figures 4a and 4b show the transition from the free-flow phase to the jammed phase as R increases. R_c's estimated from $\eta(R)$'s in Figures 4a and 4b are $R_c=24(1)$ for $(\alpha=0, x=1)$ and $R_c=54(2)$ for $(\alpha=-1/4, x=3/4)$. The value of R_c does not depend on N as in the case of $\alpha+1<x$. Measured R_c's are nearly equal to the theoretical values $R_c\simeq25(3)$ for $(\alpha=0, x=1)$ and $R_c\simeq53(1)$ for $(\alpha=-1/4, x=3/4)$. The theoretical values are obtained from $R_c=ca^{-1}$ with $(c=0.2, a=0.008(1))$ and $(c=0.133, a=0.0025(1))$, respectively.

Figure 4c shows $m(k)$ with $(\alpha=0, x=1)$ for $R=24(\simeq R_c)$ and $N=10^4$ at $t=10^5, 1.5\times10^5, 2\times10^5$, and 2.5×10^5. Unlike the cases of $x>\alpha+1$ and $x<\alpha+1$, the condition $C(k)>m(k)$ breaks on all nodes and the jamming occurs on all nodes. The stacked packets on all nodes increase as t increases. $m(k)$ thus increases for all k with t. In contrast, $m(k)$'s for $R<R_c$ satisfy the relation $m(k)=m_f(k)=aRk^{\alpha+1}$ very well as shown in the insets of Figure 4c. The data in Figure 4d for $(\alpha=-1/4, x=3/4)$ shows the same behavior as for the case in Figure 4c.

This jamming pattern also occurs for $R>R_c$ as shown in Figures 4e and 4f. As R increases, $m(k)$ for all k increases. For $R>R_c$, the increment of $m(k)$ is nearly the same for all k except for $k\simeq k_{\min}$. The anomalous increment for $k\simeq k_{\min}$ in Figures 4e and 4f is originated from the large fluctuation of the stacked packets due to the small node capacity $C(k\simeq k_{\min})$. Thus, the simulation results with $(\alpha=0, x=1)$ and $(\alpha=-1/4, x=3/4)$ verify the conjectured jamming pattern for the case of $\alpha+1=x$ in the previous section. We also confirm the conjectured pattern for $\alpha+1=x$ by the simulations with $(\alpha=-1, x=0)$ and $(\alpha=1, x=2)$. If this type of

jamming pattern arises in the real network traffic, the capacity $C(k)$ of all nodes should be enhanced more to avoid the jamming.

5 Summary

We study the jamming patterns in the traffic model in which each movable packet hops to one of the neighboring nodes with probability proportional to k^α and disappears at the target node. Since the packet forwarding capacity of a node is closely correlated to the underlying topology in real communication network, we assign the node capacity to the node with degree k as $C(k) \sim k^x$. The effect of $C(k)$ on the jamming pattern is investigated. In this model, we can exactly determine the jamming patterns from the competition between the node capacity, $C(k)$, and the average number of packets on a node, $m_f(k)$, in the free-flow phase. From the analytic arguments, we find that there are three different jamming patterns depending on $C(k)$ and $m_f(k)$. When $\alpha + 1 > x$, the jamming pattern is that the jamming for a given $R(> R_c)$ occurs on the nodes with $k \geq k_>(R)$ or with the higher degree. The order parameter scales as $\eta(R) = f(R/N^\beta)$ $(\beta = (x - \alpha - 1)/(\gamma - 1))$. Especially, at $R = R_c^+$, the traffic congestion begins to occur on the hub node with $k = k_{\max}$ and $m_f(k) \sim cN^\beta k^{\alpha+1}$. The jamming pattern at $R = R_c^+$ is the same as the condensation in zero range process [23] on complex networks. In contrast, when $\alpha + 1 < x$, the jamming pattern is that the jamming for a given R $(>R_c)$ occurs on the nodes with $k \leq k_<(R)$ or with the lower degree. On the other hand, when $\alpha + 1 = x$, the packets are stacked on all nodes in the network if $R > R_c$. These specific jamming patterns depending on the heterogeneous node capacity $C(k) = ck^x$ have never been suggested in the researches of traffic model.

These results provide a complete set of scenario to understand how the jamming occurs in real communication networks and how the traffic congestion spreads over the network as R increases. Therefore, in practice, our results can be directly applied to the prediction of the traffic congestion and can suggest wise ways to avoid the traffic jams in the real communication networks by specifying vulnerable nodes to increase their capacities.

This work was supported by National Research Foundation of Korea (NRF) Grant funded by the Korean Government (MEST) (Grant No. 2011-0015257) and by Basic Science Research Program through the National Research Foundation of Korea (NRF) funded by the Ministry of Education, Science and Technology (No. 2012R1A1A2007430).

References

1. S.-H. Yook, H. Jeong, A.-L. Barabási, Proc. Natl. Acad. Sci. **99**, 13382 (2002)
2. R. Albert, H. Jeong, A.-L. Barabási, Nature **401**, 103 (1999)
3. J.M. Kleinberg, Nature **406**, 845 (2000)
4. Q. Lv, P. Cao, E. Cohen, K. Li, S. Shenker, in *ICS'02: Proc. of the 16th ACM Intl. Conf. Supercomputing* (2002), Vol. 84
5. S. Nandi, L. Brusch, A. Deutsch, N. Ganguly, Phys. Rev. E **81**, 061124 (2010)
6. S. Lee, S.-H. Yook, Y. Kim, Physica A **385**, 743 (2007)
7. S. Lee, S.-H. Yook, Y. Kim, Phys. Rev. E **80**, 017102 (2009)
8. L.A. Adamic, R.M. Lukose, A.R. Puniyani, B.A. Huberman, Phys. Rev. E **64**, 046135 (2001)
9. K. Kim, B. Kahng, D. Kim, Europhys. Lett. **86**, 58002 (2009)
10. H. Kawamoto, A. Igarashi, Physica A **391**, 895 (2012)
11. C.H. Kai, J. Long, X. Ling, M.-B. Hu, Physica A **401**, 174 (2014)
12. W.-X. Wang, B.-H. Wang, C.-Y. Yin, Y.-B. Xie, T. Zhou, Phys. Rev. E **73**, 026111 (2006)
13. C.-Y. Yin, B.-H. Wang, W.-X. Wang, T. Zhou, H.-J. Yang, Phys. Lett. A **351**, 220 (2006)
14. B. Tadić, S. Thurner, G.J. Rodgers, Phys. Rev. E **69**, 036102 (2004)
15. L. Zhao, Y.-C. Lai., K. Park, N. Ye, Phys. Rev. E **71**, 026125 (2005)
16. S. Yoon, S. Lee, S.-H. Yook, Y. Kim, Phys. Rev. E **75**, 046114 (2007)
17. Z. Eisler, J. Kertész, Phys. Rev. E **71**, 057104 (2005)
18. S. Hwang, D.-S. Lee, B. Kahng, Phys. Rev. Lett. **109**, 088701 (2012)
19. S. Hwang, D.-S. Lee, B. Kahng, Phys. Rev. E **85**, 046110 (2012)
20. J. Gómez-Gardeñes, V. Latora, Phys. Rev. E **78**, 065102(R) (2008)
21. Z. Burda, J. Duda, J.M. Luck, B. Waclaw, Phys. Rev. Lett. **102**, 160602 (2009)
22. R. Sinatra, J. Gómez-Gardeñes, R. Lambiotte, V. Nicosia, V. Latora, Phys. Rev. E **83**, 030103(R) (2011)
23. J.D. Noh, G.M. Shim, H. Lee, Phys. Rev. Lett. **94**, 198701 (2005)
24. A. Barrat, M. Barthélemy, R. Pastor-Satorras, A. Vespignani, Proc. Natl. Acad. Sci. **101**, 3747 (2004)
25. S. Kwon, S. Yoon, Y. Kim, Phys. Rev. E **77**, 066105 (2008)
26. S. Kwon, W. Choi, Y. Kim, Phys. Rev. E **82**, 021108 (2010)
27. A. Arenas, A. Díaz-Guilera, R. Guimerá, Phys. Rev. Lett. **86**, 3196 (2001)
28. D. De Martino, L. Dall'Asta, G. Bianconi, M. Marsili, Phys. Rev. E **79**, 015101(R) (2009)
29. S.N. Dorogovtesv, J.F.F. Mendes, Adv. Phys. **51**, 1079 (2002)
30. A.-L. Barabási, R. Albert, Science **286**, 509 (1999)